

# Computational Fluid Dynamics (CFD) Flow Simulation on UiTM's Hawkeye UAV Aircraft's Airfoil Design

N. Aishah Asmizi -1\*, Zurriati M. Ali -2, M. Syazwan Johari -3  
School of Mechanical Engineering, College of Engineering,  
Universiti Teknologi MARA 40450 Shah Alam  
\*zurriatimohdali@uitm.edu.my

## ABSTRACT

*Unmanned Aerial Vehicle (UAV) aircraft with forward – swept wing configuration can fly at a low speed while maintaining excellent performance as it allows reduction in compressibility effects at transonic speed. The UiTM 'Hawkeye' UAV aircraft from previous study shows a good result which has a low in drag coefficient but low in lift coefficient, which results a low lift – to – drag [L/D] ratio of the whole aircraft. This paper discussed the aerodynamic forces characteristic; lift, drag and moment coefficient [ $C_L$ ,  $C_D$ ,  $C_M$ ] for the UAV aircraft using two types of airfoils which are CLARK – Y and NACA 2415. A Computational Fluid Dynamics (CFD) simulation using ANSYS Fluent has been used in this study. The Spalart–Allmaras turbulence model was used in this study as it is based on Reynolds Average Navier – Stokes (RANS) single equation model, thus reducing the computational time needed to run the simulation. At a flight condition of Mach number 0.1 (~35m/s), the angle of attacks for the UAV aircraft with NACA 2415 and CLARK – Y airfoil shows a similar data trend for  $C_D$ ,  $C_L$  and  $C_M$ . However, the UAV aircraft with CLARK – Y airfoil shows the best L/D ratio when compared to NACA 2415. At  $\alpha = 0^\circ$ , the UAV aircraft with NACA 2415 airfoil result  $C_L = 0.0619$ , where for CLARK – Y obtained  $C_L = 0.0981$ . As from the result obtained, it shows that CLARK – Y gives the best aerodynamic forces when compared to NACA 2410 and NACA 2415.*

**Keywords:** UAV; Forward-Swept Wing; Aerodynamics; Airfoil; CFD

## Introduction

Forward – swept wing aircraft are unusual to be seen flying in the air, but the forward – swept wing aircraft offer more advantages over the tapered or backward – swept wing [1], [2]. In comparison to aircraft with tapered or backward – swept wing design, a forward – swept wing overcome some of the problem that may arise on such aircraft. Based on few studies, a forward – swept wing done better for reducing in compressibility effect at transonic speeds while also providing much more lift at lower speed when compared to backward – swept wing aircraft [3], [4]. The issue on tip stall which is commonly happened in backward – swept aircraft can also be avoided as a result of the fluid flow from the wing tips to the root of the aircraft [5]. It will not be possible to lose control even when the air separates away from the ailerons at this point [6]. The used of a forward – swept wing design would enable any UAV aircraft fly at a low speed while maintaining excellent performance [7], [8].

A study by C.J Egeh [9] shows that aerodynamic forces characteristic; lift, drag and moment coefficient of an aircraft is dependent on the wing design. It is possible to determine aerodynamic characteristics, by having dimensionless value of the coefficient of lift,  $C_L$ , the coefficient of drag,  $C_D$  and the coefficient of moment,  $C_M$ , either by conducting wind tunnel tests or by conducting analytical analysis and simulation [10]. In a variety of studies that have been carried out, the conclusion has been reached that forward – swept wing aircraft have excellent aerodynamic characteristics [11], [12], [13]. Besides, previous work done by J. Pathak and Andrzej [14] on aerodynamics of low – speed vehicles has also shown that the CLARK – Y airfoil is one of the better airfoil designs for low speed and low drag coefficient vehicles.

The aerodynamic characteristic of any UAV aircraft can be determined easily using a Computational Fluid Dynamics (CFD) simulation software. ANSYS Fluent is one of the software that can be used to simulate variety of numerical approaches within a specific boundary and the fluid flow around a specified model. The Spalart – Allmaras (S – A), a Reynolds Average Navier – Stokes (RANS) single equation is used in this study. The S-A is a numerical approach that uses a single equation differential system for the eddy viscosity parameter and an algebraic formula to specify the length scale [15]. S-A has been proven to be numerically well behaving in most cases as it provides economical computations pf boundary layer in external aerodynamics [16], [17]. Many applications of of S-A are focused on the fully turbulent flows, where the flow is basically turbulent everywhere when vortices can be found [18], [19]. There is much applicability for the S-A turbulence model in the aerospace, including application to three – dimensional supersonic complex configurations and high subsonic flow [20].

The UiTM Research Team have built the first 'Hawkeye' UAV aircraft which using the forward – swept wing design. An initial study about the aerodynamic characteristics of the UAV aircraft using the forward – swept wing design with NACA 2410 airfoil has been performed. From the previous study, it shows that the UAV aircraft result a poor lift and moment coefficient [21]. It is possible to determine the changes to the wing design of the aircraft by using two different airfoil which are NACA 2415 and CLARK – Y airfoil to obtain better aerodynamic forces characteristics. As can be seen in Figure 1, the prototype of the 'Hawkeye' UAV aircraft was created by previous study without the involvement of the aerodynamic studies. The swept angle from the prototype has been identified based on finding from other design studies and was fixed on the UAV aircraft, thus the aerodynamic data of this UAV aircraft is unavailable.

The objective of this study is to obtain better aerodynamic forces characteristic; lift, drag and moment coefficient of the 'Hawkeye' UAV aircraft while applying the forward – swept wing design using NACA 2415 airfoil and CLARK – Y airfoil.



Figure 1: UiTM 'Hawkeye' UAV aircraft

## Methodology

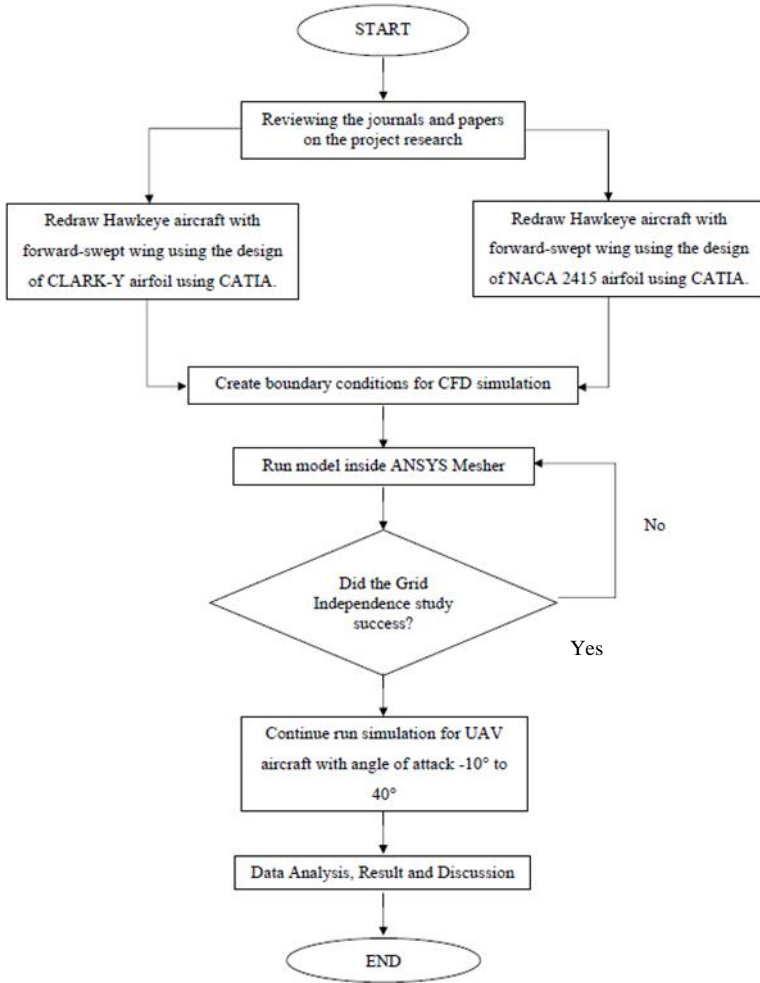


Figure 2: Process Flowchart

### Preparation of CAD Drawing

The design of the UAV aircraft has followed the previous study dimension. For the wing part, the design of airfoil has been changed to selected airfoil which are NACA 2415 and CLARK – Y. The drawing of the aircraft was prepared using the 3D Computer – Aided Design (CAD) software CATIA V5. The completed CAD drawing are then saved and converted into STP file

(.stp) before proceeding to the pre – processing stage in ANSYS Fluent. There are two types of CAD drawing that has been done in this stage which are the UAV aircraft with NACA 2415 airfoil and CLARK – Y airfoil. Table 1 describe the parameters used in the UAV aircraft. Descriptions of CAD drawing are as below.

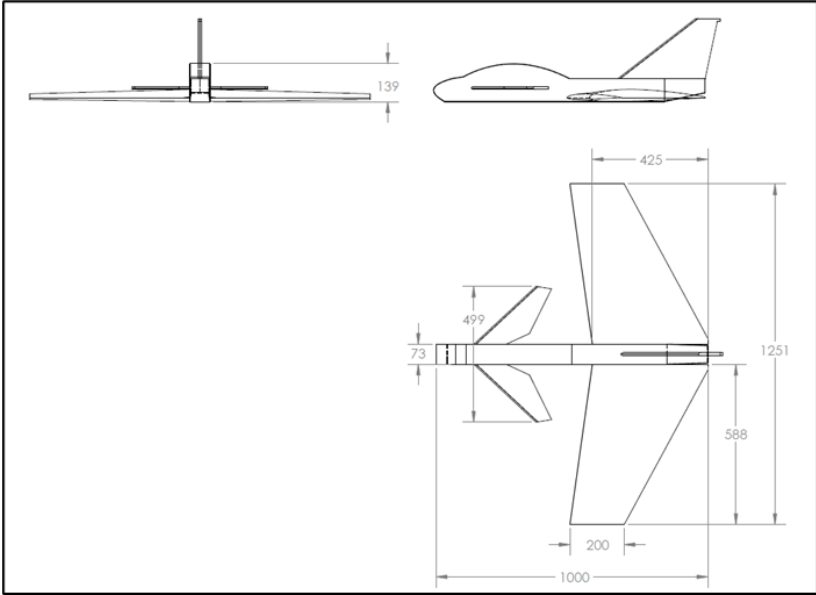


Figure 3: Drawing of UAV aircraft with NACA 2415 airfoil (full scale)



Figure 4: CLARK – Y airfoil

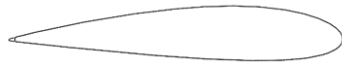


Figure 5: NACA 2415 airfoil

Table 1: UAV aircraft half model parameters

Parameters	Hawkeye Model
Area, A (m <sup>2</sup> )	0.86
Span, S (m)	2
Chord, C (m)	0.43
Moment Centre (x,y,z)	(0.15,0,0) m

### CFD Setup

ANSYS Fluent has been used for the CFD simulation on this study. The airspeed used is 35m/s which around 0.1 Mach number and the simulation will be conducted at a various angle of attacks from  $-10^{\circ}$  to  $40^{\circ}$  with an interval of  $2^{\circ}$ . Since the aircraft has the symmetrical design, the simulation only run on the half – body of the UAV aircraft. The simulation has been completed in a relatively short time when only half of the symmetrical model is included in the boundary condition setup.

### Pre – Processing

The first step of any simulation is to define a computational domain which is a complement for the UAV aircraft. The domain dimension is shown in Figure 6 and covers only half of the body of UAV aircraft. This domain is deign based on study by N. I. Ismail [22].

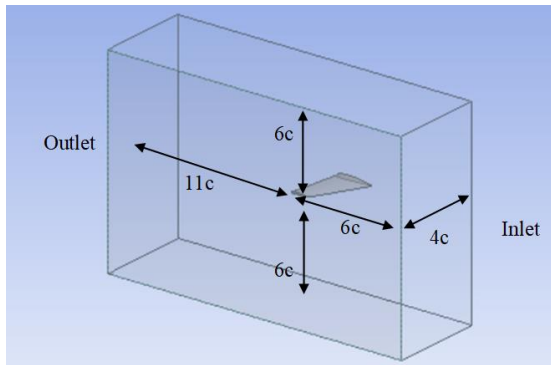


Figure 6: Computational domain for this study

Accuracy and convergence of the computed result basically depends on a good quality of mesh. ANSYS Mesher has been used to mesh the geometry of the aircraft. As shown in Figure 7, the meshed structure of half body of the UAV aircraft has been illustrated.

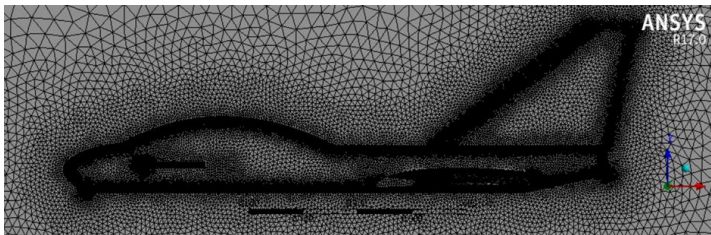


Figure 7: Half body of UAV aircraft after meshing

**Processing**

Processing stage will be performed in ANSYS Fluent software. It is important to set up project parameters before starting the simulation. Air in fluid model setting is being selected because it is important to inspect as it will affect the Reynold number in the calculation. The simulation uses the Spalart – Allmaras turbulent model for CFD analysis. Reference parameter for the half body of the UAV aircraft were stated as shown in Table 2.

Table 2: Reference parameter table

Parameters	Value
Density, $\rho$ (kg/m <sup>3</sup> )	1.17
Velocity, V (m/s)	35
Viscosity, $\mu$ (kg/m-s)	1.7894e-05
Reynold's Number	2.47 x 10 <sup>6</sup>

**Post – Processing**

By using the ANSYS Fluent simulation, the physical simulation of the fluid flow around the aircraft is completed. Through this process, the function helps to visualise the result obtained by showing the flow of air around the aircraft and give valid data.

**Validation**

A grid independence study was performed to observe the sensitivity of meshing cells toward computational results. The successful meshing sensitivity study is when the computational result becomes independent towards meshing cells. As shown in Figure 8, the grid independence study was found converged at 300,002 number of elements.

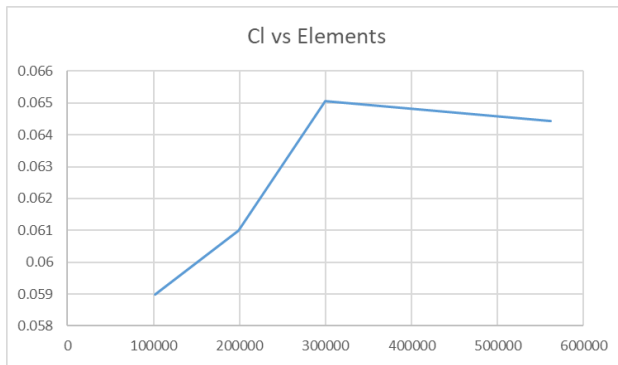


Figure 8: Grid independence study result

Parameter validation is done by validating the CFD simulation data and the wind tunnel result. This is to proof that the theoretical CFD data has the closest value to the wind tunnel experimental data.

The lift coefficient vs angle of attack graph is shown in Figure 9. The result for both CFD and wind tunnel shows similar trend but the stall angle for wind tunnel test shows a bit early at  $\alpha = 20^\circ$ , while CFD stall angle is at  $\alpha = 36^\circ$ . This is due to the sizing of the model in wind tunnel used is only 40% than the original size. This might effect the difference in Reynold number used and the data trend obtained between CFD and wind tunnel test.

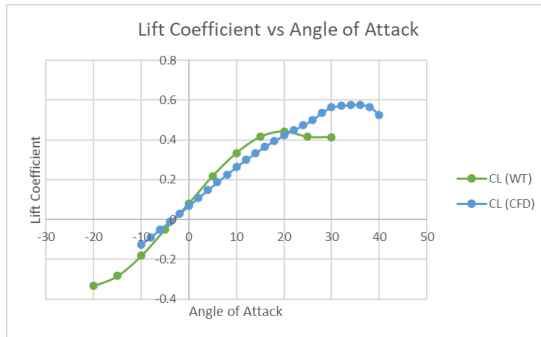


Figure 9: Lift Coefficient vs Angle of Attack

The drag coefficient vs angle of attack graph is shown in Figure 10. Both graph of wind tunnel and CFD simulation show the drag coefficient data trend is similar to each other when the drag coefficient is increased as the angle of attack increases. At  $\alpha = 10^\circ$ , it shows that the maximum deviation is only about 4%. Overall, the data obtained is reliable as the error is less than 20%.

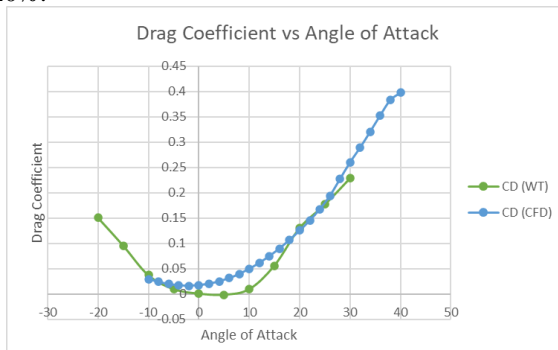


Figure 10: Drag Coefficient vs Angle of Attack



## Result and Analysis

In this study, the result computed by the CFD simulation will be compared with previous study [21]. A simple comparison on the data trends for every airfoil; NACA 2410, NACA 2415 and CLARK – Y will be discussed.

### Lift Coefficient, $C_L$ analysis

The result of the simulation on the lift coefficient against the angle of attack is shown in Figure 11. From the graph, all three airfoils have almost similar trend of  $C_L$ . This can be seen that the data shows a linear trend until it reaches the maximum lift coefficient. It can be seen at the angle of attack,  $\alpha = 36^\circ$  for CLARK – Y airfoil, the lift coefficient reached the maximum level at  $C_{Lmax} = 0.5911$ . As for NACA 2410, the  $C_{Lmax} = 0.5789$  can be seen at the angle of attack  $\alpha = 34^\circ$  and  $C_{Lmax} = 0.5772$  at  $\alpha = 36^\circ$ . Thus, the aircraft pointing to the stall angle as the lift coefficient reached the maximum level for all airfoils.

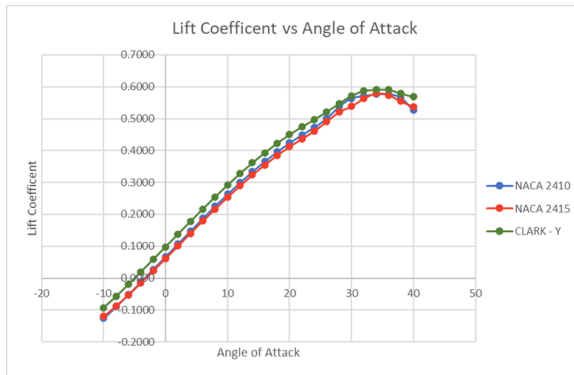


Figure 11: Lift Coefficient comparison between CLARK – Y, NACA 2415 and previous study airfoil NACA 2410

### Drag Coefficient, $C_D$ analysis

As shown in Figure 12 below, the drag coefficient computed by the CFD simulation showed a parabolic trend decreasing or increasing angles of attack, the drag coefficient will be higher for all the three airfoils. During maximum lift at  $\alpha = 40^\circ$  for CLARK – Y airfoil, the drag coefficient is  $C_{dmax} = 0.4269$ . The lowest drag coefficient experienced by the aircraft is  $C_{dmin} = 0.018$  at  $\alpha = 0^\circ$ . As for drag coefficient on NACA 2415 airfoil, during maximum lift at  $\alpha = 40^\circ$ , the drag coefficient is  $C_{dmax} = 0.4036$ . The lowest drag coefficient experienced by the aircraft is  $C_{dmin} = 0.019$  at  $\alpha = 0^\circ$ . The computed drag coefficient of the 'Hawkeye' UAV aircraft with using the CLARK – Y airfoil showed a better characteristic as compared to NACA

2410 and NACA 2415 airfoil. At an angle of  $\alpha = 0^\circ$ , the drag coefficient of ‘Hawkeye’ UAV aircraft with CLARK – Y is  $C_{dmin} = 0.018$  compared to NACA 2410 with  $C_{dmin} = 0.019$  and  $C_{dmin} = 0.019$  for NACA 2415.

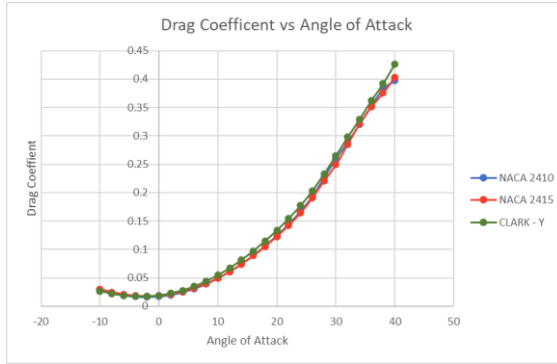


Figure 12: Drag Coefficient comparison between CLARK – Y, NACA 2415 and previous study airfoil NACA 2410

### Moment Coefficient, $C_M$ analysis

All of the ‘Hawkeye’ UAV aircraft with different airfoils showed a near similar data trend with the computed CFD, but with a much higher minimum and maximum value. As can be seen in Figure 13, UAV aircraft with CLARK – Y have a much steeper negative slope, compared to the other two airfoil which are NACA 2410 and NACA 2415. This proves that the ‘Hawkeye’ UAV aircraft with CLARK – Y airfoil have a much higher tendency to correct itself.

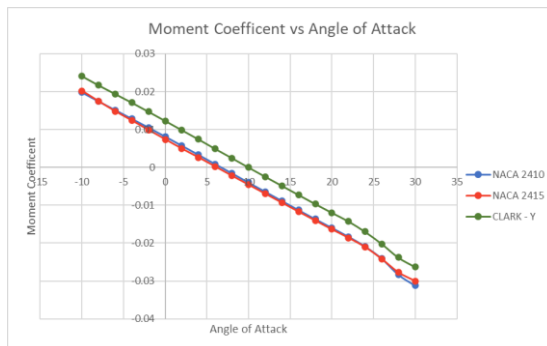


Figure 13: Moment Coefficient comparison between CLARK -Y, NACA 2415 and previous study airfoil NACA 2410

### Lift – to – Drag ratio, L/D analysis

Due to having a much higher amount of lift, the ‘Hawkeye’ UAV aircraft with CLARK – Y have a much better lift-to-drag ratio by having a maximum ratio of 6.35 compared to 5.66 and 5.97 achieved from the ‘Hawkeye’ UAV aircraft with NACA 2415 airfoil and previous study airfoil NACA 2410 CFD test. The data trend as seen in Figure 14 showed slight similarity between all the airfoil, but clearly shows that the ‘Hawkeye’ UAV aircraft with CLARK – Y have the best lift-to-drag ratio.

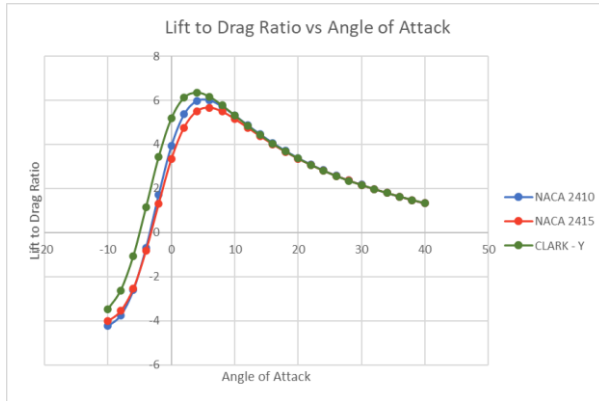


Figure 14: Lift to drag comparison between CLARK – Y, NACA 2415 and previous study airfoil NACA 2410

### Conclusion

The CFD analysis for the ‘Hawkeye’ UAV aircraft with using forward – swept wing configuration for NACA 2415 and CLARK – Y airfoil has been completed. The aerodynamic forces characteristics: lift, drag and moment coefficient were successfully obtained through CFD simulation and plotted against angle of attacks. The results that have been obtained from the simulation on each configuration shows that ‘Hawkeye’ UAV aircraft with CLARK – Y airfoil gives the highest value of lift coefficient  $C_L = 0.5911$ , the best value of moment coefficient  $C_M = -0.0262$ , the lowest value of drag coefficient,  $C_D = 0.018$  and good lift – to – drag ratio  $L/D = 6.35$  when compared to NACA 2415 and NACA 2410 airfoil.

## Recommendation

Based on the results obtained, there are some recommendations that can be suggest for future improvement. Firstly, based on this study, the change of airfoil does not seem to give a big effect on the aerodynamic characteristic of the aircraft. It is possible to change either the design of the wing, whether using a taped or backward configuration. Also, by changing the size of the wing either by increasing the width or the length and the area of the wing can possibly result much different in comparison of aerodynamic characteristic obtained for lift and drag coefficient. Besides, the use of Spalart – Allmaras turbulence only is not enough to compare the data simulation. In future, it is suggested to run the simulation using other turbulence model such as K-Epsilon to investigate the effectiveness of simulation run. Hopefully, future study can be done in other way to achieve better results for future improvement.

## References

- [1] A. Bouilloux-Lafont, A. Naronikar, N. Prakash, and S. Vijayaraghavan, “Forward Swept Wings,” in *TMAL02 Expert Conference*, 2017, vol. 24, no. 2, pp. 13–14. Accessed: Nov. 10, 2022.
- [2] M. Bertella, L. G. Sánchez, C. J. Navarro, and G. P. Magán, “Forward swept wing,” in *TMAL02 Expert Conference*, 2018, vol. 25, no. 3, pp. 13–15. Accessed: Nov. 10, 2022.
- [3] E. J. Saltzman and J. W. Hicks, “In-Flight Lift-Drag Characteristics for a Forward-Swept Wing Aircraft (and Comparisons With Contemporary Aircraft),” *NASA Technical Paper 3414*, p. 60, 1994.
- [4] F. Lundvall, W. Yachnin, J. Perroud, and K.-D. Läßle, “Forward-swept Wings,” in *TMAL02 Expert Conference*, 2019, vol. 8, no. 4, pp. 11–13. Accessed: Nov. 11, 2022.
- [5] C. Breitsamter and B. Laschka, “Vortical Flowfield Structure at Forward Swept-Wing Configurations,” *Journal of Aircraft*, vol. 38, no. 2, pp. 193–207, May 2001, doi: 10.2514/2.2758.
- [6] R. Xue, Z. Ye, and K. Ye, “Active aeroelastic wing application on a forward swept wing configuration,” *Engineering Applications of Computational Fluid Mechanics*, vol. 13, no. 1, pp. 1063–1079, Jan. 2019, doi: 10.1080/19942060.2019.1663264.
- [7] M. Y. Meddaikar, J. Dillinger, M. Ritter, and Y. Govers, “Optimization & Testing of Aeroelastically-Tailored Forward Swept Wings,” *International Forum on Aeroelasticity and Structural Dynamics*, 2017.
- [8] A. Tawfeeq and M. A. Baghdad, “Use of Panel Method in High

- Subsonic and Transonic Aerodynamic Analysis of Complex Aircraft Configuration,” *International Journal of Novel Research in Electrical and Mechanical Engineering*, vol. 5, pp. 19–29, 2017, Accessed: Nov. 11, 2022.
- [9] C. J. Ejeh, G. P. Akhabue, E. A. Boah, and K. K. Tandoh, “Evaluating the influence of unsteady air density to the aerodynamic performance of a fixed wing aircraft at different angle of attack using computational fluid dynamics,” *Results in Engineering*, vol. 4, p. 100037, Dec. 2019, doi: 10.1016/J.RINENG.2019.100037.
- [10] P. Panagiotou, P. Kaparos, and K. Yakinthos, “Winglet design and optimization for a MALE UAV using CFD,” *Aerospace Science and Technology*, vol. 39, pp. 190–205, Dec. 2014, doi: 10.1016/J.AST.2014.09.006.
- [11] N. Wang, X. Su, B. Ma, and X. Zhang, “Numerical Study on Influence of Canard Height on Aeroelastic Behavior of Forward-Swept Wing,” in *IOP Conference Series: Materials Science and Engineering*, Dec. 2018, vol. 452, no. 4, pp. 379–385. doi: 10.1088/1757-899X/452/4/042048.
- [12] H. M. Jaffal, A. S. Darwish, and I. A. Hassan, “Theoretical and Experimental Study of a Forward Swept Wing,” *Anbar Journal for Engineering Sciences*, vol. 3, no. 2, pp. 15–30, Dec. 2010, doi: 10.37649/AENGS.2010.14202.
- [13] S. Xinbing, J. Wen, and Z. Xiwei, “Study on the Influence of Swept Angle on the Aerodynamic Characteristics of the Cross-Section Airfoil of a Variable Swept-Wing Aircraft,” in *IOP Conference Series: Materials Science and Engineering*, Nov. 2019, vol. 685, no. 1. doi: 10.1088/1757-899X/685/1/012016.
- [14] J. Pathak and A. Sobiesiak, “An aerodynamic study and design methodology for the 2009 supermileage body,” *ASME International Mechanical Engineering Congress and Exposition, Proceedings*, vol. 9, no. PART C, pp. 2189–2196, 2010, doi: 10.1115/IMECE2009-10569.
- [15] A. Ali Pasha, K. A. Juhany, and M. Khalid, “Numerical prediction of shock/boundary-layer interactions at high Mach numbers using a modified Spalart–Allmaras model,” *Engineering Applications of Computational Fluid Mechanics*, vol. 12, no. 1, pp. 459–472, Jan. 2018, doi: 10.1080/19942060.2018.1451389.
- [16] C. I. Ursachi, M. C. Galbraith, S. R. Allmaras, and D. L. Darmofal, “Output-based adaptive rans solutions using higher-order fem on a multi-element airfoil,” *AIAA AVIATION 2020 FORUM*, vol. 1 PartF, pp. 1–23, 2020, doi: 10.2514/6.2020-3220.
- [17] M. M. Rahman, “Introducing Consistently Formulated Eddy-Viscosity Coefficient with Spalart–Allmaras Model,” *AIAA Journal*, vol. 58, no. 6, pp. 2764–2769, Mar. 2020, doi: 10.2514/1.J059118.

- [18] A. Medina, M. Rockwood, D. J. Garmann, and M. R. Visbal, "Integration of experiments and computations of swept-wing dynamic stall," *AIAA Scitech 2019 Forum*, 2019, doi: 10.2514/6.2019-2324.
- [19] F. Gand and M. Huet, "On the generation of turbulent inflow for hybrid RANS/LES jet flow simulations," *Computers & Fluids*, vol. 216, p. 104816, Feb. 2021
- [20] M. Mesbah, V. G. Gribin, and K. Souri, "Evaluation of different turbulence models in simulating the subsonic flow through a turbine blade cascade," *IOP Conference Series: Materials Science and Engineering*, vol. 1092, no. 1, p. 012064, Mar. 2021, doi: 10.1088/1757-899X/1092/1/012064.
- [21] M. Syazwan Johari, Z. M. Ali, W. Wisnoe, N. Ismail, and I. S. Ishak, "Computational Aerodynamic Analysis of UiTM's Hawkeye UAV Aircraft," *Journal of Aeronautics, Astronautics and Aviation*, vol. 53, no. 2, pp. 295–302, Jun. 2021, doi: 10.6125/JOAAA.202106\_53(2).23.
- [22] N. I. Ismail, A. H. Zulkifli, R. J. Talib, H. Yusoff, and M. A. Tasin, "Vortex structure on twist-morphing micro air vehicle wings," *International Journal of Micro Air Vehicles*, vol. 8, no. 3, pp. 194–205, Sep. 2016.